ISBN: 978-3-95450-236-3 ISSN: 2673-7027 doi:10.18429/JACoW-eeFACT2022-TUYAT0102

FCC-ee LATTICE DESIGN

J. Keintzel*, A. Abramov, M. Benedikt, M. Hofer, K. Oide,
R. Tomás, F. Zimmermann, CERN, Geneva, Switzerland
P. Hunchak, University of Saskatchewan, Saskatoon, Canada
T. O. Raubenheimer, SLAC National Accelerator Laboratory, USA

Abstract

Within the framework of the Future Circular Collider Feasibility and Design Study, the design of the electron-positron collider FCC-ee is being optimised, as a possible future double collider ring, currently foreseen to start operation during the 2040s. FCC-ee is designed to operate at four different energy stages, allowing for precision measurements: from the Z-pole up to above the $t\bar{t}$-threshold. This synchrotron with almost 100 km circumference is designed including advanced accelerator concepts, such as the crab-waist collision scheme or one combined off-momentum and betatron collimation insertion. Furthermore, numerous optics tuning and measurement studies are being performed to drive the collider design at an early stage and guarantee its feasibility and efficient operation.

INTRODUCTION

The Future Circular electron positron Collider [1], FCC-ee, is the first part of the so-called integrated FCC program [2], which foresees, first, the construction of an almost 100 km long tunnel infrastructure and the integration and commissioning of the FCC-ee. After completion of its physics program, it is then envisaged to decommission the FCC-ee, followed by integration of the hadron FCC [3], FCC-hh, into the same tunnel infrastructure. First collisions are presently foreseen in the mid-2040s for the FCC-ee and around 2065 for the FCC-hh [4].

A flexible high energy electron-positron collider such as the FCC-ee, offers the potential for high precision physics experiments at various particle physics resonances [5, 6]. In case of the FCC-ee beam energies from 45.6 GeV, corresponding to the Z-pole, and up to above the top-pair-threshold with 182.5 GeV are foreseen. To limit the synchrotron radiation (SR) power to 50 MV per turn the beam current decreases with increasing energy. Each energy stage leads, therefore, to unique beam dynamics challenges, and solutions need to be found in accordance with the general layout.

Within the framework of the FCC feasibility study, launched in 2021, it is aimed to provide a self-consistent design of the required technical infrastructure and the accelerator complex for the FCC-ee by end of 2025 with a mid-term review in mid-2023 [7, 8].

REVISED PLACEMENT

The tunnel infrastructure required to host the FCC in the Geneva basin is assumed to be constructed approximately 100 m below ground, similar to the tunnel which presently hosts the Large Hadron Collider, LHC [9]. Tunnel construction is one of the main cost drivers, and depends on the tunnel dimensions, depth and composition of the ground material. Additionally, shafts and surface sites around the circumference are required to host various infrastructures, demanding dedicated civil engineering solutions. Geographic constraints to integrate a circular collider into the Franco-Swiss-Basin are the various mountain ranges surrounding it, including the Jura-mountains in the north-west and the Plateau des Bornes in the south-east in addition to the Geneva lake in the north-east. Furthermore, a possible circular tunnel should surround the Salève-mountain and, hence, these constraints already limit the circumference to about 80 km to 100 km.

Considering all described constraints it has been found that a 90 km tunnel with a four-fold symmetry together with 8 surface sites and straight sections is the most suitable layout. Figure 1 shows the FCC and the LHC placement schematically. The FCC-hh and the FCC-ee lattices have, therefore, been adapted to follow this new tunnel infrastructure and the latter is described in the following.

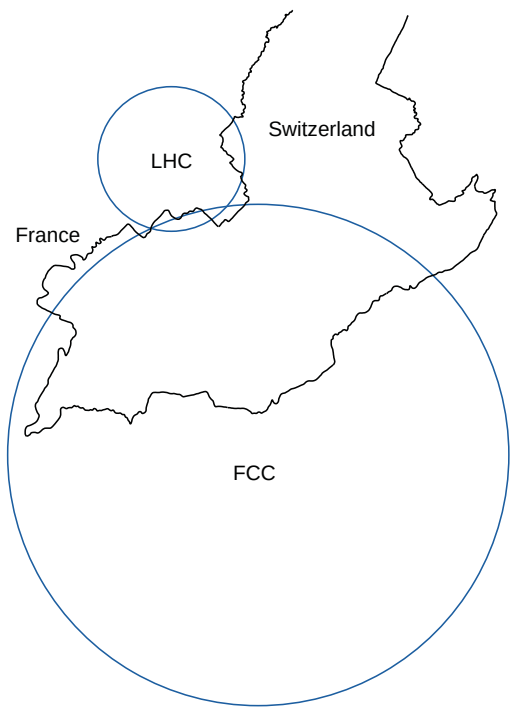

Figure 1: Comparison between the LHC, the FCC and the Franco-Swiss border.

* jacqueline.keintzel@cern.ch

ISBN: 978-3-95450-236-3 ISSN: 2673-7027 doi:10.18429/JACoW-eeFACT2022-TUYAT0102

Table 1: Latest FCC-ee beam optics parameters for the lattice with four interaction points [12].

		Z	WW	ZH	$t\bar{t}$
Circumference	[km]	91.174			
Bending radius	[km]	9.937			
SR power per beam	[MW]	50			
Half crossing angle	[mrad]	15			
Beam Energy	[GeV]	45.6	80	120	182.5
Beam Current	[mA]	1280	135	26.7	5.0
Bunches/beam	[-]	10000	880	248	40
Bunch population	[10^{11}]	2.43	2.91	2.04	2.37
Horizontal emittance	[nm]	0.71	2.16	0.64	1.49
Vertical emittance	[pm]	1.42	4.32	1.29	2.98
Arc cell phase advance	[°]	90/90			
Arc cell length	[m]	100		50	
Momentum compaction factor	[10^{-6}]	28.5		7.33	
Arc sextupole families	[-]	75		146	
Betatron tunes	[-]	214.260 / 214.380		402.224 / 394.360	
Synchrotron tune	[-]	0.0370	0.0801	0.0328	0.0826
β_x^* / β_y^*	[mm]	100 / 0.8	200 / 1.0	300 / 1.0	1000 / 1.6
Energy spread with SR/BS	[%]	0.038 / 0.132	0.069 / 0.154	0.103 / 0.185	0.157 / 0.221
Bunch length with SR/BS	[mm]	4.38 / 15.4	3.55 / 8.01	3.34 / 6.00	1.95 / 2.75
RF-frequency	[MHz]	400	400	400	400 + 800
Total RF voltage	[GV]	0.120	1.0	2.08	11.25
Long. damping time	[turns]	1168	217	64.5	18.5
Energy acceptance	[%]	±1.3	±1.3	±1.7	−2.8 +2.5
Luminostiy / IP	[10^{34} cm^{-2}s^{-1}]	182	19.4	7.26	1.25
Polarization time	[s]	15000	900	120	4.6
SR losses/turn	[GeV]	0.039	0.370	1.869	10.0

GENERAL LAYOUT

Compared to the FCCC-ee CDR version numerous changes have been made, including a shorter circumference and the possibility of integrating four instead of two experiments [11]. The FCC-ee lattice follows the new, so-called lowest risk tunnel scenario with approximately 91.1 km circumference, eight straight sections, (PA, PB, PD, PF, PG, PH, PJ and PL) and is schematically shown in Fig. 2. It offers the possibility of up to four experimental insertion regions (IRs) in PA, PD, PG and PL, where the beams are brought to collision from the inside outwards. Thus, beams are required to change from the inside to the outside aperture in all IRs. The beam collimation section is placed in PF. RF-cavities are foreseen to be integrated in one to two IRs, PL and PH. The electron and the positron beams are presumed to be injected continuously at nominal beam energy in PB (top-up injection) from the High Energy Booster (HEB). The HEB is designed to be installed in the same tunnel infrastructure and thus its lattice design must also be compatible with the one for the colliding rings. Thus, the lattice design of the FCC-ee must comply with all three rings hosted in the same tunnel, and thus two IRs are dedicated for the RF-cavities of the three rings.

Designed at four different beam energies of 45.6, 80, 120 and 182.5 GeV, the FCC-ee allows for physics precision experiments at the Z-pole, the W-pair-threshold, the ZH-maximum and above the top-pair-threshold [6]. It is presently presumed to operate the FCC-ee with increasing beam energy over years, which, among others, requires a flexible lattice and optics design, allowing for fast transitions including upgrades of the RF-cavities to compensate increasing SR energy losses. The latest FCC-ee lattice and optics parameters are summarized in Table 1 [12].

ARCS

The eight arcs are designed using FODO cell structures, consisting of horizontally focusing and defocusing quadrupoles (QF and QD in the lattice) with bending dipoles in-between, with a transverse phase advance of 90° at all energy stages. Although the transverse phase advance is constant over all energies, we note that at the Z-pole and the WW-threshold the cell length is 100 m, while at ZH- and $t\bar{t}$-operation it is reduced to about 50 m by inserting additional quadrupole magnets [12]. Non-interleaved individually powered 76 or 146 sextupole pairs, respectively for the two lower or higher beam energy modes, are installed with a $-I$-transformation between them. The periodic structure within the arc, named super-cell, consists of five FODO cells and contains one focusing and one defocusing sextupole pair. Therefore also additional sextupole magnets are required to

ISBN: 978-3-95450-236-3 ISSN: 2673-7027 doi:10.18429/JACoW-eeFACT2022-TUYAT0102

be installed when switching to the shorter FODO cells arc lattice for the higher beam energies. Due to fewer quadruple magnets in the arc optics for the lower beam energies at the Z- and WW-mode, the arc β-functions are roughly a factor 2 larger and the horizontal dispersion by almost a factor 4. A schematic plot of one or two super-cells, respectively, for the lower and higher beam energy arc designs is shown in Fig. 3.

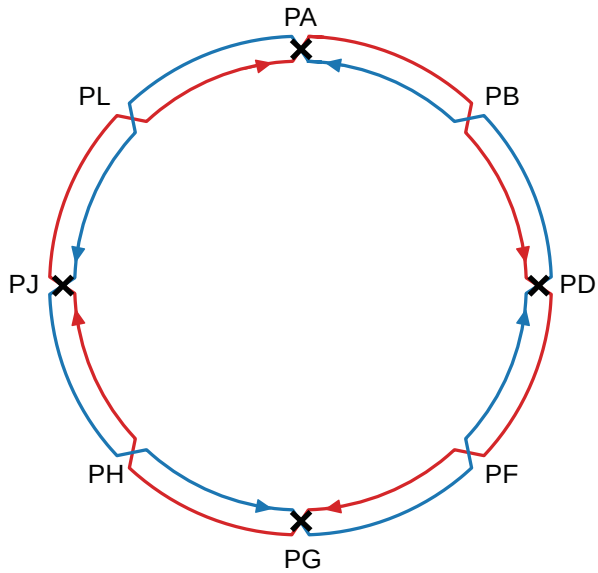

Figure 2: FCC-ee general layout with four-fold periodicity and super-symmetry with 8 straight sections. The positron and the electron beam are circulating, respectively, clock and counter-clock wise. The four experimental straight sections are marked with a black cross.

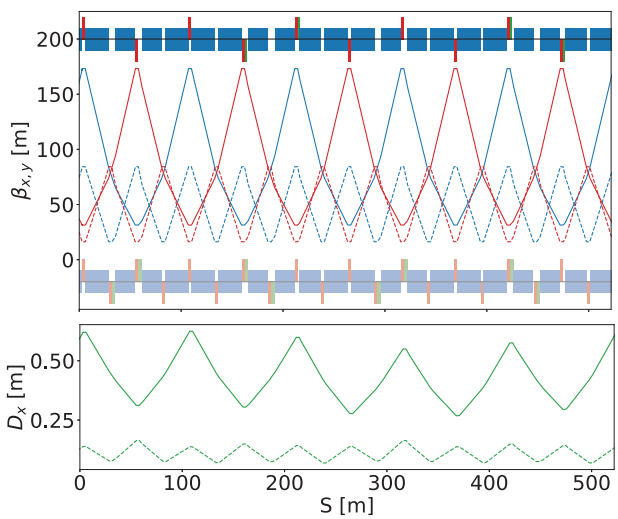

Figure 3: FCC-ee arc lattice and optics for five FODO cells (equivalent to one super-cell) for the Z- and WW-mode (solid lines); and ten FODO cells (equivalent to two super-cells) for ZH- and $t\bar{t}$-mode (dashed lines). Horizontal and vertical β-functions are shown in, respectively, blue and red. Dipoles, quadrupoles and sextupoles are shown, respectively, in blue, red and green. Focusing and defocusing elements, respectively, are shown below and above the horizontal axis.

The sextupole families are optimized to maximize the momentum aperture up to about 2.8 % at 182.5 GeV, since beamstrahlung and synchrotron radiation lead to a wide momentum spread. Additionally, horizontal on-momentum dynamic aperture of about 15 σ is achieved, required for top-up injection. The possibility of using fewer than 75 and 146 sextupole pairs, respectively, for the lower energy and higher energy operation modes, while reaching the required momentum aperture, is envisaged to be explored.

EXPERIMENTAL INSERTIONS

All four experimental IRs feature the same optics design with horizontal and vertical β-functions at the interaction point (IP) of as low as $\beta^*_{x,y} = 100, 0.8$ mm at the Z-pole, shown in Fig. 4, and a crossing angle of 30 mrad. Although β^*_y is about 3 times larger than the SuperKEKB design [13], the generated chromaticity around the IP is in the same order of magnitude for both colliders. It has to be noted, that the minimum β^*_y achieved so far in SuperKEKB is 0.8 mm and thus approximately a factor 3 larger than its design.

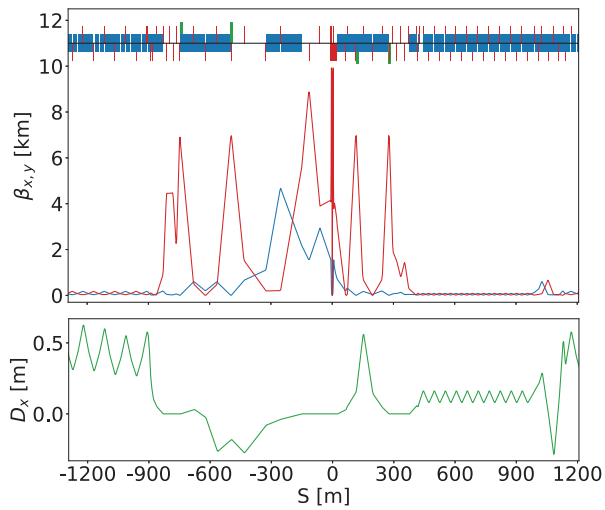

Figure 4: Lattice and optics for the experimental interaction region for the Z-pole. $S = 0$ marks the IP. Horizontal and vertical β-functions are shown in, respectively, blue and red. The beam direction is from left to right. Dipoles, quadrupoles and sextupoles are shown, respectively, in blue, red and green. Focusing and defocusing elements, respectively, are shown below and above the horizontal axis.

To control the generated chromaticity, a local chromaticity correction scheme (LCCS) consisting of non-interleaved sextupole pairs, for the vertical plane is integrated on both IP sides. The outer sextupoles of the LCCS are also the ones used for the crab-waist transformation [14–16]. For the crab-waist collision scheme vertical beam sizes in the order of a few nano-meter are brought to collision with a large Piwinksi-angle aligning the waist of the β-functions on

ISBN: 978-3-95450-236-3 ISSN: 2673-7027 doi:10.18429/JACoW-eeFACT2022-TUYAT0102

the axis of the other beam via adequate sextupole powering. The crab-waist sextupoles correspond to the outer ones of each pair and are placed at a horizontal and vertical phase advance of, respectively, 2π and 2.5π with respect to the IP on both sides, as schematically shown in Fig. 5, together with the presently used terminology of the IR quadrupoles. This scheme has first been tested successfully at DAΦNE [14–16] with dedicated crab-sextupoles and is presently also used in SuperKEKB [13] using the virtual crab-waist collision scheme which is also foreseen for the FCC-ee [5].

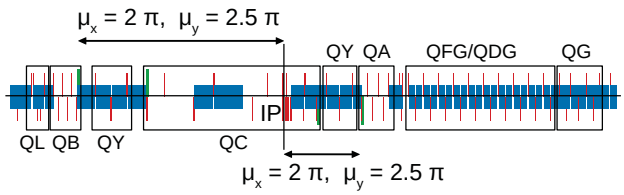

Figure 5: Betatron phase advance between the IP and the LCCS sextupoles and terminology of quadrupoles in the experimental IRs. Dipoles, quadrupoles and sextupoles are shown, respectively, in blue, red and green. Focusing and defocusing elements, respectively, are shown below and above the horizontal axis.

In each IP beams cross from the inside to the outside aperture as shown in Fig. 6, to mitigate synchrotron radiation at the detector. This requires weaker dipole magnets downstream of the IP, and stronger ones upstream of it. Since the beams are crossing from the inside aperture at all experimental IRs (PA, PD, PG and PJ), beam crossings from the outside towards the inside are required at all other straight sections (PB, PF, PH and PL). In the experimental IRs no common magnets are foreseen for the electron and the positron beam [17]. Recent progress on Machine Detector Interface (MDI) studies is being reported in [18–20].

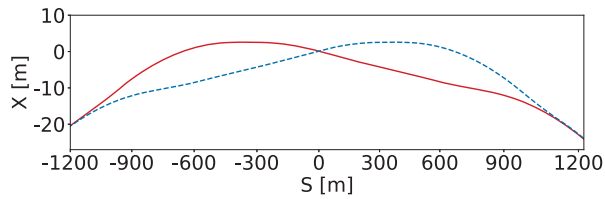

Figure 6: Beam crossing at the IP from the inner towards the outer aperture. $S = 0$ marks the IP.

INJECTION

The positron and the electron beams are injected continuously from the HEB in PB at nominal energy, known as top-up injection. One can distinguish in principle between on- and off-momentum injection, and using a conventional orbit bump or a multipole kicker injection (MKI), resulting in four possible scenarios presently investigated for the FCC-ee [21]. For multipole-kicker injection a dedicated optics has been designed and the on-momentum one is shown in

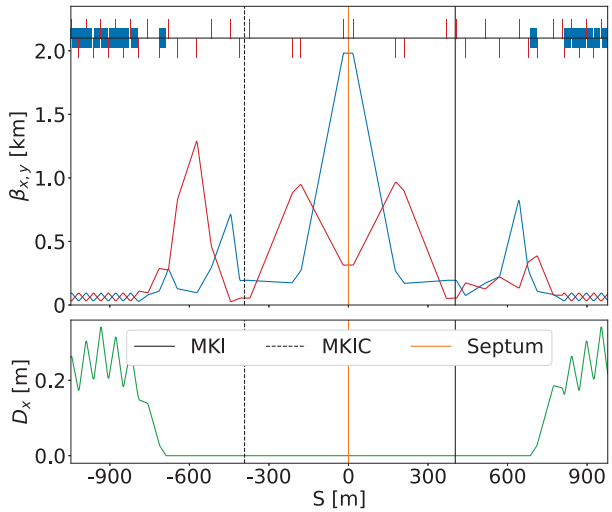

Figure 7: Optics and lattice for on-momentum injection using a multipole kicker (MKI) and a correction magnet (MKIC) for a 2-IP lattice. Horizontal and vertical β-functions are shown in, respectively, blue and red. The beam direction is from left to right. Dipoles, quadrupoles and collimators are shown, respectively, in blue, red and black. Focusing and defocusing elements, respectively, are shown below and above the horizontal axis.

Fig. 7. It features a large horizontal β-function of about 2000 m at the injection point, centered between the MKI and a corrector magnet, MKIC. Previous tracking studies have shown that by integrating an additional MKIC beam size blow-up at the IP is successfully corrected [22]. We note that this optics is optimized for the 2-IP version and significant changes for the 4-IP lattice will need to be applied [23]. Furthermore, if the RF-cavities are not located in the same IR for the HEB and the main rings, the energy saw tooth could lead to different local beam energies between the injector, the electron and the positron ring which must be considered [24]. Future studies will show the most suitable injection technique for the 4-IP FCC-ee lattice.

COLLIMATION

The stored beam energy in the FCC-ee reaches up to 20.7 MJ [25], and is, therefore, comparable to heavy ion operation at the Large Hadron Collider, LHC [10]. One collimation insertion with beam crossing in its center, is integrated into the FCC-ee lattice in PF [26]. This insertions optics, as shown in Fig. 8 for the $t\bar{t}$-mode combines halo and off-momentum collimation, located, respectively, upstream and downstream of the beam crossing. In each plane there is a two-stage collimation system, with 1 primary and 2 secondary colliamtors. While for the halo-collimation the horizontal dispersion is kept low, it reaches up to about ±0.6 m for the momentum collimation, which allows independent cuts in betatron amplitude and in momentum offset [26]. The horizontal and vertical primary collimators are set at 15 σ_x and 80 σ_y respectively, while the off-momentum

ISBN: 978-3-95450-236-3 ISSN: 2673-7027 doi:10.18429/JACoW-eeFACT2022-TUYAT0102

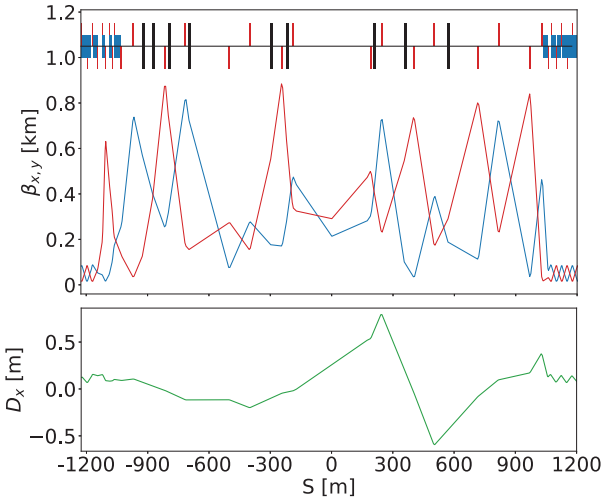

Figure 8: Optics and lattice for the collimation insertion for tt̄-mode. Betatron and off-momentum collimation are located, respectively, upstream and downstream of the beam crossing in the center, located at $S = 0$. Horizontal and vertical β-functions are shown in, respectively, blue and red. The beam direction is from left to right. Dipoles, quadrupoles and collimators are shown, respectively, in blue, red and black. Focusing and defocusing elements, respectively, are shown below and above the horizontal axis.

primary is set at 23.0 σ_x, corresponding to a dp/p cut of 2.9 %, just outside the RF bucket acceptance. The location of the collimators for tt̄-operation are also shown in the same figure.

First loss map studies for the 4-IP lattice are performed for betatron collimation at 182.5 GeV beam energy using the newly-developed Xtrack-BDSIM coupling framework [25]. 5×10^6 primary positrons are tracked for 700 turns without radiation and optics tapering, and the FCC-ee aperture model [27] is used. The resulting loss map over the circumference, assuming a molybdenum-graphite primary collimator, are shown in Fig. 9. In addition to the collimators in PF, significant warm and cold losses are also observed in the four experimental IRs. The results are preliminary and further studies, including a comparison with beam loss scenarios and equipment loss tolerances, are required to assess the performance of the collimation system.

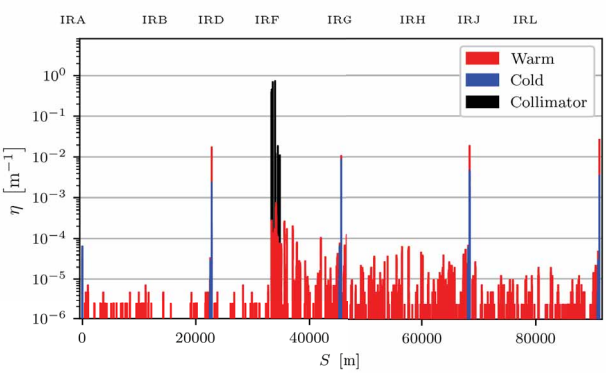

Figure 9: Loss map studies for betatron collimation for the positron ring at 182.5 GeV beam energy with $5{\times}10^6$ primary particles using a molybdenum-graphite primary collimator.

RF-INSERTIONS

Although beams are injected at the nominal energy into the main rings, energy is lost due to, for example, synchrotron radiation, beamstrahlung or longitudinal impedance sources. The present baseline foresees elliptical cavities with frequencies of 400 MHz and 800 MHz, whereby novel studies investigate the so-called slotted waveguide elliptical cavities with 600 MHz. More details can be found in [28].

Two RF-sections are presently foreseen at the highest beam energy stage and only one for all lower operation energies. Especially at the Z-pole and the WW-threshold, placing the collider RF-cavities in only one straight section is crucial for precision physics requirements [6], since this allows for keeping the center-of-mass energy, ECM, constant within a few keV at all IPs when considering losses from SR and beamstrahlung, as also demonstrated in [29]. At the Z- and the WW-operation separate RF-cavities are foreseen for the electron and the positron beam with a beam crossing in the center of the straight section. Contrarily, at the ZH- and tt̄-mode the present design has common RF-cavities and thus beams must cross before or after being accelerated. To reduce SR power on the RF-cavities only the outgoing beam is deflected [5]. The lattices and terminology of quadrupoles for the IR hosting the RF-system are shown schematically in Fig. 10 for Z- and tt̄-mode. Additionally, the optics are shown in Fig. 11.

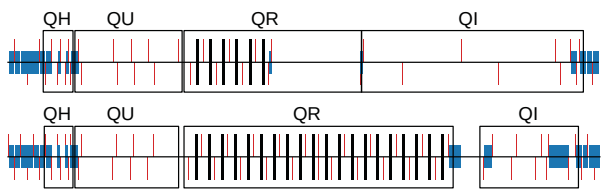

Figure 10: Terminology of quadrupoles in the RF IRs. Dipoles, quadrupoles and RF-cavities are shown, respectively, in blue, red and black. Focusing and defocusing elements, respectively, are shown below and above the horizontal axis.

ENERGY LOSSES

Severe synchrotron radiation losses in lepton storage rings lead naturally to energy losses over each turn. While for the lowest beam energy only roughly 40 MeV are lost due to SR, in case of the highest beam energy about 5.5 % (10 GeV) of the total beam energy is lost per turn. SR power losses depend on the Lorentz-factor by γ_{rel}^4 and thus, also on the local beam energy throughout the circumference. In addition to

ISBN: 978-3-95450-236-3 ISSN: 2673-7027 doi:10.18429/JACoW-eeFACT2022-TUYAT0102

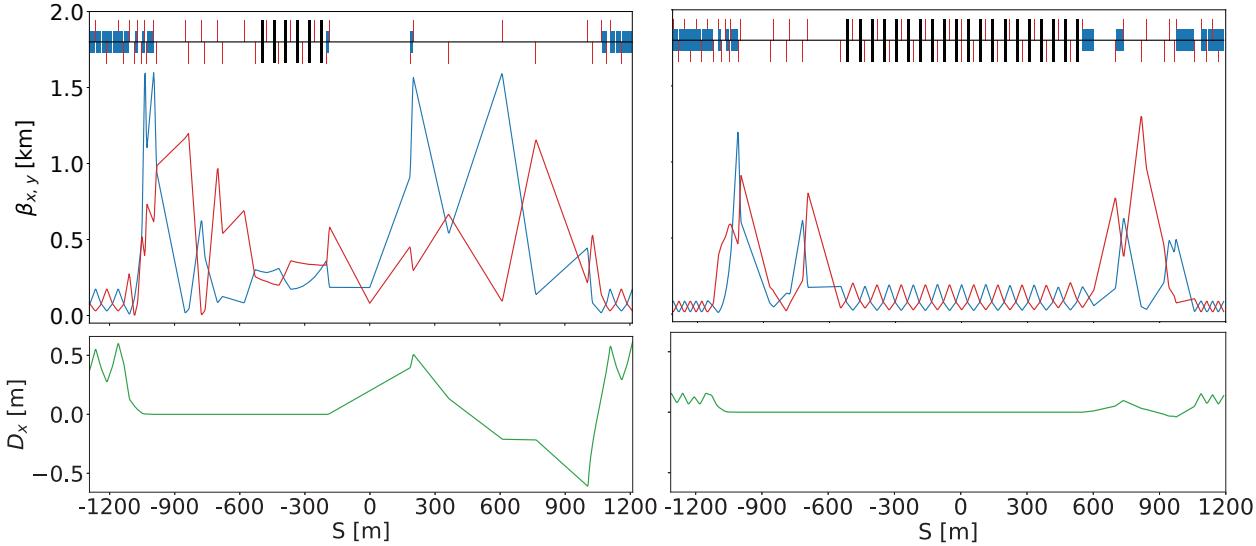

Figure 11: Optics for the RF insertion for Z- (left) and tt̄-modes (right). Horizontal and vertical β-functions are shown in, respectively, blue and red. The beam direction is from left to right. Dipoles, quadrupoles and RF-cavities are shown, respectively, in blue, red and black. Focusing and defocusing elements, respectively, are shown below and above the horizontal axis.

SR, energy losses from beamstrahlung for colliding bunches and longitudinal impedance or energy shifts due to crossing angles also impact the local beam energy. Furthermore, energy drifts are also a result of machine circumference change caused by e.g. Earth tides. All systematic energy losses must be compensated by the RF-cavities. First studies aiming to determine the beam energy over the circumference include SR and beamstrahlung losses for the positron and the electron beam. Figure 12 shows the beam energy variation for both beams without and with beamstrahlung losses at each IP of 14 MeV simulated with MAD-X. In this example two RF-sections are assumed with 400 MHz 5 GV cavities in PH and 800 MHz 6.7 GV in PL. The difference between the lowest and the highest beam energy is 7.56 GeV.

Without adjusting the element's strengths to the local beam energy, large orbits and optics beatings would be generated. To avoid these, the strengths of lattice elements are scaled according to the local beam energy. This is known as tapering, and is included in the lattice design [38]. While ideal tapering of all elements individually is optimal to mitigate optics aberrations, a huge number of power supplies and, possibly, corrector coils would be required.

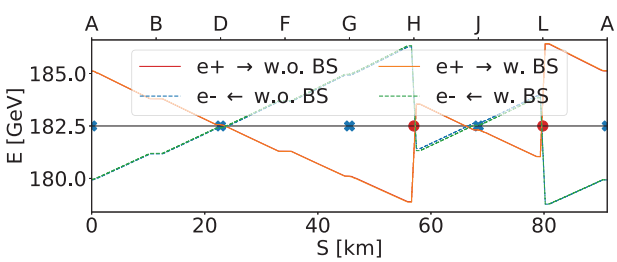

Figure 12: Beam energies at the tt̄-mode with and without beamstrahlung (BS) at the IPs for RF-sections located in PL and PH.

ENERGY CALIBRATION, POLARIZATION AND MONOCHROMATIZATION

Since the discovery potential of the FCC-ee is directly linked to the achieved precision on the ECM measurement, huge effort is put into energy calibration, polarization and monochromatization (EPOL) studies in a dedicated working group [30] and numerous reports have recently been made, e.g. in [31] and in a dedicated workshop [32]. Due to the unprecedented luminosity a statistical precision of 4 keV and 100 keV, respectively, for the Z- and the W-mass measurements is predicted [6]. It is, therefore, envisaged achieving a systematic precision in the same order of magnitude by depolarizing transversely polarized low-intensity (10^{10} particles per bunch) non-colliding pilot bunches, which requires dedicated hardware to be integrated in the lattice.

The natural polarization time is 250 h and 15 h and the Z- and WW-mode, respectively. To enhance polarization it is foreseen to integrate wiggler magnets, following the three-block design of those installed in the Large Electron Positron Collider (LEP) [33]. They are presently integrated in each experimental straight section downstream the IP in a dispersion free section (see also Fig. 4). In total 24 units providing 0.7 T magnetic field are foreseen for the FCC-ee, which reduce the polarization time to 12 h while increasing the energy spread to 64 MeV in case of the Z-pole [34]. Furthermore, the integration of wigglers leads to photon generation with a critical energy in the order of MeV and, therefore, possibly imposing radiation protection constraints.

ISBN: 978-3-95450-236-3 ISSN: 2673-7027 doi:10.18429/JACoW-eeFACT2022-TUYAT0102

Wigglers are only used to achieve up to approximately 5 to 10 % polarization on roughly 200 low intensity pilot bunches, and are switched off once this goal is fulfilled. Subsequently all nominal intensity bunches are injected and brought to collision. A transverse kicker depolarizes the pilot bunches and the impact on the polarization is measured using polarimeters.

Foreseen polarimeters are based on inverse Compton scattering processes of the beam with laser photons (532 nm wavelength) travelling in the opposite direction of the beam. Approximately 2 m are required for the Laser Interaction Region (LIR), followed by an about 2 mrad bending dipole and a 100 m long drift space. The back-scattered photons and the scattered leptons with the minimum energy are then measured with silicon-pixel detectors, allowing to reconstruct the 3D polarization vector. One suitable location would be upstream of the straight section hosting the RF-cavities, where one polarimeter for each beam could be installed. Another suitable lattice location for integration of polarimeters could also be upstream of the IP, using the last arc dipole with 1.6 mrad. However, the subsequent drift space is only roughly 50 m, which could impose reducing the laser photon wavelength by a factor 2 or could require higher resolution silicon-pixel detectors, which remains to be explored in future studies [35]. While the baseline foresees only one polarimeter per beam, it has recently been suggested investigating in the feasibility and necessity of installing one polarimeter per beam and IP [36].

TUNING STUDIES

One of the most crucial challenges of the FCC-ee is achieving the design performance for a lattice including non-homogeneous beam energy, misalignments and multipole field errors together with dedicated correction techniques. Numerous aspects are addressed in a dedicated working group, where the most recent meeting can be found in [37]. Furthermore, findings from tuning studies will also feedback into the lattice design and a few examples are given in the following.

The current FCC-ee layout does not explicitly include Beam Position Monitors (BPMs), orbit correctors or skew quadrupoles. It is assumed that orbit correctors and skew quadrupoles coils can be added to every sextupole. However current emittance tuning studies [39] assume the integration of orbit corrector magnets next to every quadrupole, which implies more than a factor 2 larger number of orbit correctors than currently foreseen by placing them at sextupoles. Preliminary simulations show that the length of the orbit correctors should be between 10 cm and 25 cm [40].

SuperKEKB has recently observed shifts of the transverse sextupoles position in the order of 10 µm due to temperature changes between low and high beam current operation [41]. Low beam current is needed for the optics tuning as this involves orbit changes around the ring. The feed-down from the sextupole shifts distorts the optics and is potentially affecting injection efficiency and luminosity. In FCC-ee Z-mode a 3 µm horizontal shift of one IR sextupole changes the vertical tune by about 5×10^{-3} units and introduces a 20 % β-beating. For arc sextupoles the required shift to generate comparable aberrations is 250 µm. The FCC-ee will therefore require accurate beam-based sextupole alignment techniques to the 1 µm level, together with the capability to measure optics aberrations at high beam currents. Notably, studies for CEPC are assuming beam-based sextupole alignment with an accuracy of 10 µm [42]. The technology to achieve these ambitious challenges should be investigated. It should include robust sextupole-to-quadrupole alignment or attaching BPMs to sextupoles should be considered.

Suitable optics measurements techniques for the FCC-ee are essential for the control of the beam optics. Turn-by-Turn (TbT) optics measurements have found to be a promising and fast solution in obtaining the beam optics for the FCC-ee [43], since they are regularly used in numerous existing circular storage rings such as the LHC [44, 45] or are presently being explored for SuperKEKB [46]. To apply existing TbT measurement techniques, the beam needs to be excited to increase the action, either by single kicks or by a continuous excitation to force betatronic oscillations. The latter could be applied during high beam current operation to one or few bunches to limit risks related to beam losses or synchrotron radiation and allowing optics tuning in parallel with luminosity production. This requires BPMs with bunch-by-bunch and TbT capabilities together with high frequency kickers which need to be allocated in the machine layout.

SUMMARY AND OUTLOOK

An updated FCC-ee lattice and optics have been designed which follow the novel tunnel layout. Hence, it features a four-fold symmetry and super-periodicity with eight IRs and the possibility of hosting up to four experiments in PA, PD, PG and PJ, where an electron and a positron beam are brought to collision. To limit the SR power on the detectors, the beams always cross from the inside towards the outside in the experimental insertions. Consequently, this demands beams crossing from the outside inwards in all auxiliary IRs. Top-up injection at the nominal energy is foreseen for both beams in PB from the high energy booster, located in the same tunnel infrastructure. Halo-collimation and betatron collimation systems are combined in PF. PL and PH are foreseen to host the RF-cavities for the main rings and the booster.

The FCC-ee optics features a large dynamic and momentum aperture, while simultaneously achieving beam sizes in the nano-meter regime at the IP. Generated chromaticity from the final focus is corrected using a local chromaticity correction in the vertical plane with sextupoles, which are also used for the virtual crab-waist collision scheme.

Complementary studies aiming to determine the ECM as precise as possible have shown the necessity for the integration of wiggler magnets and polarimeters in each beam, which have already successfully been integrated into the lattice. Lastly, tuning studies explore the best location and

ISBN: 978-3-95450-236-3 ISSN: 2673-7027 doi:10.18429/JACoW-eeFACT2022-TUYAT0102

parameters for BPMs and corrector magnets and will influence the final FCC-ee lattice design.

To conclude, great progress has been made since the CDR and the latest lattice and optics design have been shown here. Large combined effort in defining the first FCC-ee baseline design is presently ongoing, aimed to be delivered in the framework of the FCC-IS with a mid-term review in 2023 and the final report end of 2025.

ACKNOWLEDGMENTS

The work is also supported by the FCC-IS project, receiving funding from the European Union's H2020 Framework Programme under grant agreement no. 951754. Furthermore, the authors would like to that R. Bruce and G. Wilkinson for fruitful discussions and comments on the manuscript.

REFERENCES

[1] M. Benedikt *et al.* (eds.), "Future Circular Collider study, Volume 2: The Lepton Collider (FCC-ee) Conceptual Design Report", in Eur. Phys. J. ST. **228**, pp. 261–623, 2019.

[2] M. Benedikt, A. Blondel, P. Janot, M. Mangano, and F. Zimmermann, "Future circular colliders succeeding the LHC", in Nat. Phys. **16**, pp. 402–407, 2020. doi:10.1038/s41567-020-0856-2

[3] M. Benedikt *et al.* (eds.), "Future Circular Collider study, Volume 3: The Hadron Collider (FCC-hh) Conceptual Design Report", in Eur. Phys. J. ST. **228**, pp. 755–1107, 2019.

[4] F. Gianotti, "Welcome and introduction from CERN", presented at the FCC-Week 2022, Paris, France, 2022. indico.cern.ch/event/1064327/contributions/4891231/

[5] K. Oide *et al.*, "Design of beam optics for the future circular collider e+e- collider rings", Phys. Rev. Accel. Beams **19**, pp. 1111005, 2016.

[6] A. Blondel *et al.*, "Polarization and centre-of-mass energy calibration at FCC-ee", doi:arXiv:1909.12245v1, 2019.

[7] M. Benedikt and F. Zimmermann, "Future Circular Collider: Integrated Programme and Feasibility Study", Front. in Physics **10**, pp. 888078, 2022. doi:10.3389/fphy.2022.888078

[8] F. Zimmermann *et al.*, "FCC-ee Feasibility Study progress", presented at the 65th ICFA Advanced Beam Dynamics Workshop on High Luminosity Circular e+e- Colliders (eeFACT22), Frascati (RM), Italy, Sept. 2022, this workshop.

[9] O. Brüning *et al.*, "LHC Design Report", CERN, Geneva, Switzerland, Rep. No. CERN-2004-003-V-1, 2004.

[10] R. Bruce *et al.*, "Performance and luminosity models for heavy-ion operation at the CERN Large Hadron Collider", *Eur. Phys. J. Plus*. **136** pp. 745, 2021, https://doi.org/10.1140/epjp/s13360-021-01685-5

[11] J. Gutleber, "Update of the layout and placement development", presented at the FCC-Week 2022, Paris, France, 2022. indico.cern.ch/event/1064327/contributions/4888577/

[12] K. Oide "IR Optics for FCC-ee", presented at the FCC-EIC Joint & MDI Workshop 2022, 17th to 28th October 2022. indico.cern.ch/event/1186798/contributions/5062582

[13] Y. Ohnishi *et al.*, "Accelerator design at SuperKEKB", in Progr. of Theoretical and Experimental Physics, **2013** (3), 2013. doi:10.1093/ptep/pts083

[14] P. Raimondi, "Crab waist collisions in DAΦNE and Super-B design", in Proc. of Europ. Particle Accelerator Conf. (EPAC'08), Genoa, Italy, WEXG02, pp. 1898 – 1902, 2008. doi:accelconf.web.cern.ch/e08/papers/wexg02

[15] M. Zobov, "Crab waist collision scheme: a novel approach for particle colliders", in Journal of Physics: Conference Series 747, pp. 012090, 2016. doi:10.1088/1742-6596/747/1/012090

[16] M. Zobov *et al.*, "Test of crab-waist collisions at the DAΦNE Φ-factory", Phys. Rev. Let. 104, pp. 174801, 2010. doi:10.1103/PhysRevLett.104.174801

[17] M. Koratzinos *et al.*, "Status Update of the FCC-ee IR Magnet Design", presented at the 65th ICFA Advanced Beam Dynamics Workshop on High Luminosity Circular e+e- Colliders (eeFACT22), Frascati (RM), Italy, Sept. 2022, this workshop.

[18] M. Boscolo *et al.*, "FCC-ee MDI design", presented at the 65th ICFA Advanced Beam Dynamics Workshop on High Luminosity Circular e+e- Colliders (eeFACT22), Frascati (RM), Italy, Sept. 2022, this workshop.

[19] FCC-ee collaboration, "Machine detector interface workpackage", Accessed 12th October 2022. indico.cern.ch/category/5665/

[20] FCC-ee collaboration, "FCC-EIC Joint & MDI Workshop 2022", 17th to 28th October 2022. indico.cern.ch/event/1186798/

[21] R. Ramjiawan, *et al.*,"FCCee e+/e- injection and RCS booster", presented at the 65th ICFA Advanced Beam Dynamics Workshop on High Luminosity Circular e+e- Colliders (eeFACT22), Frascati (RM), Italy, Sept. 2022, this workshop.

[22] P. Hunchak, "Studies on top-up injection into the FCC-ee collider ring", in Proc. 13th Int. Part. Accel. Conf (IPAC'22), Bangkok, Thailand, WEPOST011, SUSPMF006, pp. 1699-1702, 2022. doi:10.18429/JACoW-IPAC2022-WEPOST011

[23] M. Aiba *et al.*, "Top-up injection schemes for future circular lepton collider", Nucl. Instr. Methods in Phys. Res. Sec. A, vol. **880**, pp. 98–106, 2018. doi:10.1016/j.nima.2017.10.075

[24] J. Keintzel, "Energy sawtooth due to SR and CM energy", presented at the 2nd EPOL Workshop, 19th to 30th September 2022. indico.cern.ch/event/1181966/contributions/5047163/

[25] A. Abramov *et al.*, "Development of collimation simulations for the FCC-ee", in Proc. 13th Int. Part. Accel. Conf (IPAC'22), Bangkok, Thailand, WEPOST016, pp. 1718–1721, 2022. doi:10.18429/JACoW-IPAC2022-WEPOST016

[26] M. Hofer *et al.*, "Design of a collimation section for the FCC-ee", in Proc. 13th Int. Part. Accel. Conf (IPAC'22), Bangkok, Thailand, WEPOST017, pp. 1712–1725, 2022. doi:10.18429/JACoW-IPAC2022-WEPOST017

[27] M. Moudgalya, "First studies of the halo collimation needs in the FCC-ee", Master's thesis, Department of Physics, Imperial College London, 2021.

ISBN: 978-3-95450-236-3 ISSN: 2673-7027 doi:10.18429/JACoW-eeFACT2022-TUYAT0102

[28] F. Peauger *et al.*, "Baseline & Cavity options for FCC-ee", presented at the 65th ICFA Advanced Beam Dynamics Workshop on High Luminosity Circular e+e- Colliders (eeFACT22), Frascati (RM), Italy, Sept. 2022, this workshop.

[29] J. Keintzel, A. Blondel, T.H.B. Persson, D. Shatilov, R. Tomás, F. Zimmermann, "Centre-of-Mass Energy in FCC-ee", in Proc. IPAC'22, WEPOST007, pp. 1683–1886, 2022. doi:10.18429/JACoW-IPAC2022-WEPOST007

[30] The FCC-ee collaboration, "FCC-ee energy calibration, polarization and monochromatization (EPOL) working group", Accessed 3rd October 2022. indico.cern.ch/category/8678/

[31] J. Keintzel *et al.*, "FCC-ee Energy Calibration and Polarization", submitted to Proc. of Science, Int. Conf. on High Energy Physics (ICHEP), Bologna, Italy, paper 048, 2022.

[32] The FCC-ee collaboration, "2d FCC Polarization Workshop", 19th to 30th September 2022. indico.cern.ch/e/EPOL2022

[33] J.M. Jowett and T.M. Taylor, "Wigglers for control of beam characteristics in LEP", IEEE Trans. Nucl. Sci. **30**, pp. 2581–2583, 1983.

[34] M. Hofer, "FCC-ee optics and integration of polarimeter and wigglers", presented at the 2nd FCC EPOL Workshop, 19th to 30th September 2022. indico.cern.ch/event/1181966/contributions/5041448

[35] N. Muchnoi, "Update on polarimeter precision", presented at the 5th FCC-FS EPOL group meeting, 27th January 2022. indico.cern.ch/event/1119730/contributions/4701833

[36] A. Blondel, "Summary first week and outlook for the second", presented at the 2nd FCC EPOL Workshop, 19th to 30th September 2022. indico.cern.ch/event/1181966/contributions/5041348

[37] The FCC-ee collaboration, "FCC-ee tuning WG meeting", 22nd September 2022. indico.cern.ch/event/1201405/

[38] L. van Riesen-Haupt, H. Burkhardt, R. Tomás and T.H.B. Persson, "Comparison of accelerator codes for simulation of lepton colliders", in Proc. 12th Int. Part. Accel. Conf (IPAC'21), Campinas, SP, Brazil, TUPAB004, pp. 1334–1337, 2022. doi:10.18429/JACoW-IPAC2021-TUPAB004

[39] T.K. Charles, B. Holzer, K. Oide and F. Zimmermann, "Update on the low emittance tuning of the e+/e- Future Circular Collider", in Proc. 12th Int. Part. Accel. Conf (IPAC'21), Campinas, SP, Brazil, WEPAB011, pp. 2601–2604, 2021. doi:10.18429/JACoW-IPAC2021-WEPAB011

[40] R. Tomás *et al.*, "Correction and tuning", presented at the FCC week 2022, Paris.

[41] Y. Ohnishi, "SuperKEKB optics tuning", FCC-ee tuning meeting, Aug 25th, 2022. indico.cern.ch/event/1192040/

[42] Y. Wang *et al.*, "CEPC collidering lattice design", presented at the 65th ICFA Advanced Beam Dynamics Workshop on High Luminosity Circular e+e- Colliders (eeFACT22), Frascati (RM), Italy, Sept. 2022, this workshop.

[43] J. Keintzel, R. Tomás, F. Zimmermann, "Prospects for Optics Measurements in FCC-ee", in Proc. IPAC'22, TUOZSP1, pp. 827–830, 2022. doi:10.18429/JACoW-IPAC2022-TUOZSP1

[44] R. Tomás, *et al.*, "Record low β beating in the LHC", Phys. Rev. ST Accel. Beams **15**, pp. 091001, 2012.

[45] T. Persson, F. Carlier, J. Coello de Portugal, A. Garcia-Tabares Valdivieso, A. Langner, E. H. Maclean, L. Malina, P. Skowronski, B. Salvant, R. Tomás, and A. C. Garcia Bonilla, "LHC optics commissioning: A journey towards 1% optics control", Phys. Rev. Accel. Beams, **20**, pp. 061002, 2017.

[46] J. Keintzel *et al.*, "SuperKEKB Optics Measurements Using Turn-by-Turn Beam Position Data", in Proc. 12th Int. Part. Accel. Conf (IPAC'21), Campinas, SP, Brazil, TUPAB009, pp. 1352–1355, 2021. doi:10.18429/JACoW-IPAC2021-TUPAB009